PCCP

Accepted Manuscript

ROYAL SOCIETY OF CHEMISTRY

www.rsc.org/pccp

Luminescent properties of 2-mercaptobenzothiazolates of trivalent lanthanides

Vasily A. Ilichev,[a,b] Anatoly P. Pushkarev,*[a,b] Roman V. Rumyantcev,[a] Artem N. Yablonskiy,[b,c] Tatyana V. Balashova,[a,b] Georgy K. Fukin,[a,b] Dmitry F. Grishin,[b] Boris A. Andreev,[b,c] and Mikhail N. Bochkarev[a,b]*

[a] *G. A. Razuvaev Institute of Organometallic Chemistry of Russian Academy of Sciences, Tropinina 49, 603950 Nizhny Novgorod, Russian Federation.*

E-mail: ilichev@iomc.ras.ru; pushkarev@iomc.ras.ru; Fax: +7 (831) 4627497; Tel: +7 (831) 4627709.

[b] *Nizhny Novgorod State University, Gagarina avenue 23/2, 603950 Nizhny Novgorod, Russian Federation.*

[c] *Institute for Physics of Microstructures of Russian Academy of Sciences, 7 ul. Akademicheskaya, 603950 Nizhny Novgorod, Russian Federation.*

Abstract

A series of lanthanide complexes (Ln = Nd, Sm, Eu, Gd and Yb) with anionic 2-mercaptobenothiazolate (mbt) ligands were synthesized. Depending on solvent chosen for the synthesis complexes $Ln(mbt)_3(THF)_2$ and $Ln(mbt)_3(Et_2O)$ were precipitated from THF and Et_2O solution respectively. Structure of $Yb(mbt)_3(Et_2O)$ was determined by X-ray analysis. Photophysical properties of the complexes were studied. It was found that under photoexcitation Nd and Yb derivatives exhibit bright metal-centered luminescence in NIR region while $Sm(mbt)_3(THF)_2$ demonstrates intensive visible emission corresponding to $^4G_{5/2} \rightarrow {}^6H_J$ (J = 5/2, 7/2, 9/2, 11/2) f-f transitions of Sm^{3+} along with NIR emission of moderate intensity. In the case of europium compounds as well as $Sm(mbt)_3(Et_2O)$ no luminescence was detected. It is assumed that difference in photoluminescence of Yb and Eu complexes can be explained by intramolecular electron transfer process which efficiently proceeds in these compounds.

Introduction

In recent decades lanthanide complexes with organic ligands have been attracting great attention as advanced optical materials for progressive technologies due to its useful practical applications in telecommunications, OLED-devices, solar energy conversion, as well as in bio-sciences.[1-4] It was shown by Weissman that ligands in organolanthanides play role of antenna to harvest and transmit the excitation energy to lanthanide ion.[5] Extremely low absorption coefficients of free trivalent lanthanide ions specified by forbidden character of f-f transitions tends to use

chromophore ligands implementing efficient energy transfer towards lanthanide ion. To describe energy transfer two different mechanisms are commonly discussed. The first one was proposed by Forster and considers dipole-dipole interaction between donor (D) and acceptor (A) which are located at a distance of 50-100 Å. The probability per second of energy transfer from D to A in this case is given by:

$$P_{dd}(R) = \frac{3c^4\hbar^4\sigma_A}{4\pi n^4 \tau_D R^6} \int \frac{f_D(E) F_A(E)}{E^4} dE \qquad (1)$$

where R is the separation between D and A, n is the refractive index, σ_A is the absorption cross-section of A, τ_D is the radiative lifetime of D, $f_D(E)$ and $F_A(E)$ represent normalized spectral line shape of the D emission and A absorption.[6] The second one is Dexter's which determines the energy transfer probability of quantum mechanical exchange interaction between two closely located centers (distance is shorter than 10 Å) as:

$$P_{ee}(R) = (2\pi/\hbar) K^2 exp(-2R/L) \int f_D(E) F_A(E) dE \qquad (2)$$

Here, K^2 is a constant with dimension of energy squared and L is an effective Bohr radius.[6] Despite differences in energy transfer phenomenon both theories take into account overlapping of the D emission and A absorption spectra. According to Fermi's golden rule total probability of resonant energy transfer W_{DA} is determined also by perturbation operator H':

$$W_{DA} = (4\pi^2/h) \left| \langle D^* A | H' | D A^* \rangle \right|^2 \Omega_{DA} \qquad (3)$$

where Ω_{DA} is the spectral overlap integral, H' is defined by the nature of occurring energy transfer.[7]

Mentioned theoretical approaches adequately describe luminescent properties of a wide range of lanthanide compounds.[8] Since the process of energy transfer from triplet ($^3T_1$) excited state of ligand to resonant level of Ln^{3+} ion has the highest probability hence overlapping between ligand phosphorescence and metal ion absorption bands plays key role in photoluminescence (PL) of organolanthanides.[9] This concept was specified by empirical rule which states that efficient energy transfer in lanthanide based organic materials occurs when the energy difference between $^3T_1$ state of ligand and resonant level of Ln^{3+} ion is around 2500-3500 cm^{-1}.[3] It is known that Yb^{3+} ion has one low-lying resonant energy level (≈ 10400 cm^{-1}) therefore its luminescence can be sensitized only by ligands with relatively low energy $^3T_1$ excited state. Nevertheless there are numerous complexes of ytterbium which demonstrate metal-centered emission in the case of noncompliance with empirical rule and even zero spectral overlapping Ω_{DA}.[10-12] In order to explain this phenomenon an alternative mechanism of energy transfer in ytterbium containing systems was proposed by Horrocks et al.[13] The mechanism postulates reduction of Ln^{3+} by excited organic ligand to Ln^{2+} ion and formation of intermediate state consisting of divalent

lanthanide and cation-radical ligand. Back electron transfer from Ln^{2+} towards cation-radical ligand results in formation of anionic ligand and excited Yb^{3+*} ion which subsequently emits light. It was assumed also that the same redox process is responsible for absence of any luminescence in case of some europium complexes. The thermodynamic probability of the photoinduced electron transfer depends on redox properties of lanthanide-ligand pair as:

$$\Delta G_{ET} = e_0 \left(E_{ox} - E_{red} \right) - \mathrm{E}_S - w \qquad (4)$$

where E_{ox} and E_{red} are the redox potentials of ligand and lanthanide respectively, E_S is the $^1S_0$ excited state energy and w is the stabilization energy of ion pair.[14] Consequently, only for Eu, Yb and probably Sm having high Ln^{3+}/Ln^{2+} electrode potentials[15] reduction process is possible. According to substantially developed theory of charge transfer (CT) electronic transitions in coordination compounds of transition metals[16] ligands exhibiting reducing properties are eligible. For the purpose of investigation how low-energy ligand to metal charge transfer (LMCT) state can affect on luminescent properties of Ln^{3+} ion complexes of Nd, Sm, Gd, Eu and Yb with 2-mercaptobenzothiazolate ligand were synthesized and studied.

Methods

General procedures

All manipulations were carried under vacuum using standard Schlenk techniques. The complexes $Ln[N(SiMe_3)_2]_3$ were synthesized according to the procedure published elsewhere.[17] 2-Mercaptobenzathiazole was purchased from Aldrich. The C, H, N elemental analyses were performed by the Microanalytical laboratory of IOMC on Euro EA 3000 Elemental Analyzer. The lanthanide content was analyzed by complexometric titration. IR spectra were obtained on a Perkin Elmer 577 spectrometer and recorded from 4000 to 450 cm^{-1} as a Nujol mull on KBr plates. UV–Vis absorption spectra were performed in 1 cm vacuum stopcock cell and recorded on a «Perkin-Elmer Lambda-25» from 200 to 800 nm. Emission spectra of solid samples were registered from 400 to 1500 nm on Ocean Optics USB2000 and NIR512 spectrometers.

Synthesis

Synthesis of $Nd(mbt)_3(THF)_2$ (1). A solution of $Nd[N(SiMe_3)_2]_3$ (122 mg, 0.20 mmol) in THF (5 ml) was added to a solution of mercaptobenzothiazole (98 mg, 0.59 mmol) in THF (5 ml). The reaction mixture was stirred for 30 min at the room temperature. The solution was concentrated to 2 ml. The precipitate of complex **1** was landed of hexane, separated by decantation, washed with cold hexane and dried in vacuum. Yield 127 mg (83%). Anal. Calcd. (%) for $C_{29}H_{28}N_3NdO_2S_6$ (787.18): C, 44.25; H, 3.59; N, 5.34; Nd, 18.32; S, 24.44. Found (%): C, 44.29; H, 3.55; N, 5.40; Nd, 18.37; S, 24.48. IR (ν, cm^{-1}): 1597 (w), 1430 (m), 1390 (s), 1341 (w), 1320

(m), 1285 (w), 1250 (m), 1155 (w), 1130 (w), 1080 (s), 1029 (s), 1014 (s), 933 (w), 870 (m), 752 (s), 727 (m), 671 (m), 606 (w).

In a similar manner were obtained the complex:

$Yb(mbt)_3(THF)_2$ (8). From mercaptobenzothiazole (123 mg, 0.74 mmol) and $Nd[N(SiMe_3)_2]_3$ (160 mg, 0.25 mmol). Yield 166 mg (83%). Anal. Calcd. (%) for $C_{29}H_{28}N_3O_2S_6Yb$ (815.98): C, 42.69; H, 3.46; N, 5.15; S, 23.58; Yb, 21.21. Found (%): C, 42.62; H, 3.44; N, 5.18; S, 23.60; Yb, 21.27.

The IR spectrum of 8 is identical to that of **1**.

The details of **$Sm(mbt)_3(THF)_2$ (3)**, **$Eu(mbt)_3(THF)_2$ (5)** and **$Gd(mbt)_3(THF)_2$ (7)** synthesis were published elsewhere.[18]

Synthesis of $Nd(mbt)_3(Et_2O)$ (2). To a solution of $Nd[N(SiMe_3)_2]_3$ (100 mg, 0.16 mmol) in 5 ml Et_2O a solution of mercaptobenzothiazole (80 mg, 0.48 mmol) in 5 ml Et_2O was added. The reaction mixture was stirred for 30 min at the room temperature. The precipitate of complex **2** was separated by decantation, washed with cold Et_2O and dried in vacuum. Yield 100 mg (87%). Anal. Calcd. (%) for $C_{25}H_{22}N_3NdOS_6$ (717.09): C, 41.87; H, 3.09; N, 5.86; Nd, 20.11; S, 26.83. Found (%): C, 41.89; H, 3.05; N, 5.90; Nd, 20.17; S, 26.88. IR (ν, cm^{-1}): 1597 (w), 1430 (m), 1390 (s), 1341 (w), 1320 (m), 1285 (w), 1250 (m), 1155 (w), 1130 (w), 1124 (m), 1080 (s), 1029 (s), 1014 (s), 933 (w), 870 (m), 752 (s), 727 (m), 671 (m), 606 (w).

In a similar manner were obtained the complexes:

$Sm(mbt)_3(Et_2O)$ (4). From mercaptobenzothiazole (66 mg, 0.39 mmol) and $Sm[N(SiMe_3)_2]_3$ (83 mg, 0.13 mmol). Yield 81 mg (85%). Anal. Calcd. (%) for $C_{25}H_{22}N_3OS_6Sm$ (723.21): C, 41.52; H, 3.07; N, 5.81; S, 26.60; Sm, 20.79. Found (%): C, 41.55; H, 3.10; N, 5.83; S, 26.67; Sm, 20.82.

$Eu(mbt)_3(Et_2O)$ (6). From mercaptobenzothiazole (86 mg, 0.51 mmol) and $Eu[N(SiMe_3)_2]_3$ (108 mg, 0.17 mmol). Yield 106 mg (86%). Anal. Calcd. (%) for $C_{25}H_{22}EuN_3OS_6$ (724.82): C, 41.43; H, 3.06; Eu, 20.97; N, 5.80; S, 26.54. Found (%): C, 41.40; H, 3.07; Eu, 21.01; N, 5.83; S, 26.58.

$Yb(mbt)_3(Et_2O)$ (9). From mercaptobenzothiazole (58 mg, 0.35 mmol) and $Yb[N(SiMe_3)_2]_3$ (75 mg, 0.11 mmol). Yield 73 mg (85%). Anal. Calcd. (%) for $C_{25}H_{22}N_3OS_6Yb$ (745.89): C, 40.26; H, 2.97; N, 5.63; S, 25.79; Yb, 23.20. Found (%): C, 40.24; H, 2.95; N, 5.68; S, 25.74; Yb, 23.23.

The IR spectra of **4, 6, 9** are identical to that of **2**.

X-Ray

The X-ray diffraction data for **9** were collected on an Agilent Xcalibur Eos diffractometer (Mo-K_α radiation, ω-scan technique, λ = 0.71073 Å, T = 100(2) K). The structure **9** was solved by

direct methods and refined on F^2 using SHELXTL[19] package. All non-hydrogen atoms were found from Fourier syntheses of electron density and were refined anisotropically. All hydrogen atoms were placed in calculated positions and were refined in the riding model ($U_{iso}(H)$ = $1.5U_{eq}(C)$ in CH_3-groups and $U_{iso}(H)$ = $1.2U_{eq}(C)$ in other groups). SCALE3 ABSPACK (CrysAlis Pro)[20] was used to perform area-detector scaling and absorption corrections. CCDC-1034673 contains the supplementary crystallographic data for this paper. These data can be obtained free of charge from the Cambridge Crystallographic Data Centre via www.ccdc.cam.ac.uk/conts/retrieving.html.

Crystal data for complex **9**: M= 745.85, monoclinic crystal system, space group $P2_1/c$, a= 8.07021(10) Å, b= 19.1975(3) Å, c= 17.7338(2) Å, β= 93.6245(11)º, V= 2741.97(6) Å^3, Z=4, d_{calc}= 1.807 mg·m^{-3}, μ= 3.893 mm^{-1}, $F(000)$= 1468, reflections collected/unique = 47245/6601, R_{int}= 0.0494, S(F^2) = 1.012, $R1$= 0.0210 and $wR2$= 0.0417 for $I>2\sigma(I)$, R1 = 0.0292 and $wR2$= 0.0417 for all data, largest diff. peak and hole 0.499 / -0.515 e·Å^{-3}.

Time resolved spectroscopy

The PL decay times were measured under pulsed excitation with a third harmonic of a Spectra-Physics Nd:YAG laser at 355 nm (pulse duration – 10 ns). The PL signal was dispersed with a grating spectrometer Acton-2300 and detected with a cooled InP/InGaAs-based PMT Hamamatsu H10330A-75 in the IR range (900-1500 nm), or with a Si-based PMT in the visible range (450-800 nm).

Results and discussion

Synthesis and structure

The 2-mercaptobenzothiazolate lanthanide complexes $Ln(mbt)_3(THF)_2$ and $Ln(mbt)_3(Et_2O)$ (Ln = Nd, Sm, Eu, Gd, Yb) for investigation of their photophysical properties were synthesized from the corresponding $Ln[N(SiMe_3)_2]_3$ and 2-mercaptobenzothiazole (Scheme 1).

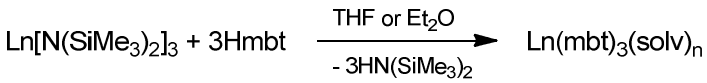

$Ln(mbt)_3(THF)_2$: Ln = Nd (**1**); Ln = Sm (**3**); Ln = Eu (**5**); Ln = Gd (**7**); Ln = Yb (**8**).
$Ln(mbt)_3(Et_2O)$: Ln = Nd (**2**); Ln = Sm (**4**); Ln = Eu (**6**); Ln = Yb (**9**).

Scheme 1. Synthesis of lanthanide 2-mercaptobenzothiazolates **1**-**9**.

The compounds have different colour depending on Ln^{3+} ion and coordinated solvent molecules: Alice blue (**1**,**2**); light yellow (**3**); cream (**4**); maroon (**5**); violet (**6**); white (**7**); yellow (**8**); amber (**9**). Their poor air stability requires utilizing of a vacuum technique for absorption and PL

measurements. In the case of Yb derivative (**9**) suitable crystals for X-ray analysis were obtained.

The X-ray investigation of complex **9** revealed that the Yb atom is coordinated by one Et_2O molecule and three flat mbt ligands (Fig. 1). Each mbt ligand in **9** coordinates to the metal centre in η^2 -fashion via N and exocyclic S atoms. Two of mbt ligands lay factually in the same plane (dihedral angle between these mbt ligands is 6.7°) while the third one is orthogonal to them (dihedral angles between the ligands planes are 91.3 and 89.2°). The similar disposition of mbt ligands takes place in previously published $Sc(mbt)_3(THF)$ compound.[21] In distinct from **9** and $Sc(mbt)_3(THF)$ three mbt ligands in related complexes $Ln(mbt)_3(THF)_2$ (Ln= Eu, Tb, Er)[20,22] form a propeller like structure. Such difference is caused by coordination of two THF molecules on the metal centre in Eu, Tb and Er compounds as compared to coordination of only one molecule Et_2O in **9** or THF in Sc derivative. Apparently smaller size of coordination sphere of Yb^{3+} and Sc^{3+} cations as compared with Eu^{3+}, Tb^{3+} and Er^{3+} ones prevents the coordination of the second molecule of solvent that leads to noticeable differences in coordination environment between them. The geometrical parameters of the mbt ligands in all complexes are close to each other. The Yb-N and Yb-S distances in **9** vary in the range of 2.3206(16)-2.4231(16)Å and 2.7432(5)-2.7700(5) Å and some exceed analogous distances in Sc complex (Sc-N: 2.216(3)-2.266(3) Å; Sc-S: 2.6632(10)-2.7034(9) Å). This is agreed with difference in ionic radii between Yb^{3+} (R_{ion}(CN=7)=0.925 Å) and Sc^{3+} (R_{ion}(CN=6)=0.745 Å; R_{ion}(CN=8)=0.87 Å) cations.[23]

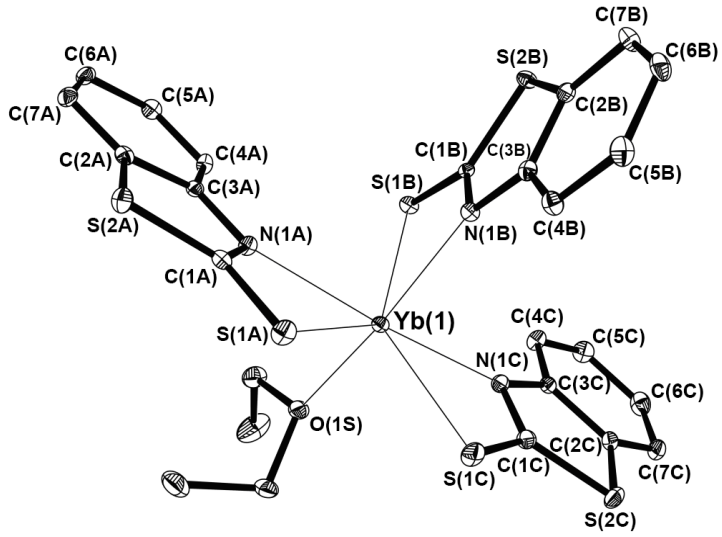

Fig. 1. Molecular structure of $Yb(mbt)_3(Et_2O)$ with 30% ellipsoid probability. Hydrogen atoms are omitted for clarity. Selected bond lengths (Å): Yb(1)-O(1S) 2.3029(14), Yb(1)-N(1A)

2.4120(16), Yb(1)-N(1B) 2.3206(16), Yb(1)-N(1C) 2.4231(16), Yb(1)-S(1A) 2.7613(5), Yb(1)-S(1B) 2.7700(5), Yb(1)-S(1C) 2.7432(5), S(1A)-C(1A) 1.719(2), S(2A)-C(1A) 1.747(2), S(2A)-C(2A) 1.7490(19), N(1A)-C(1A) 1.328(2), N(1A)-C(3A) 1.399(2), S(1B)-C(1B) 1.7182(19), S(2B)-C(2B) 1.7459(19), S(2B)-C(1B) 1.7483(19), N(1B)-C(1B) 1.326(2), N(1B)-C(3B) 1.399(2), S(1C)-C(1C) 1.716(2), S(2C)-C(1C) 1.754(2), S(2C)-C(2C) 1.755(2), N(1C)-C(1C) 1.322(2), N(1C)-C(3C) 1.408(2).

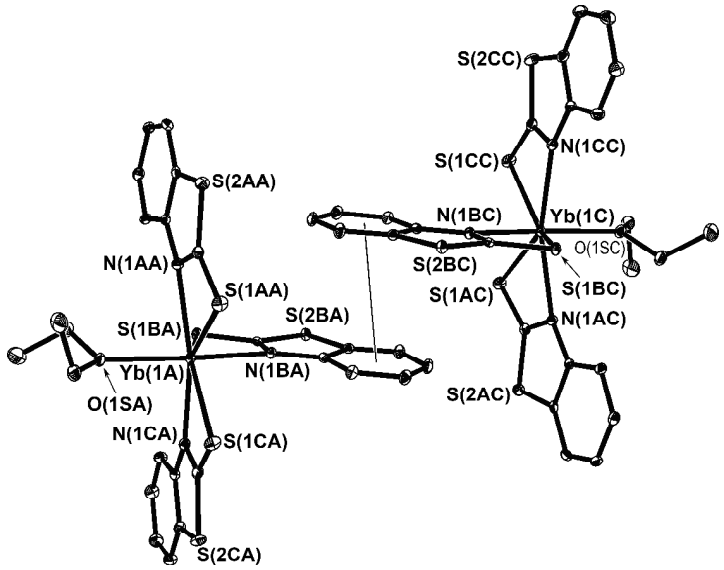

Fig. 2. Fragment of crystal packing of $Yb(mbt)_3(Et_2O)$.

The molecules of complex **9** form a dimer pairs in crystal on account of π…π interactions between mbt ligands (Fig.2). The distance between centers of six-membered fragments of mbt ligands is 3.643 Å and the planes of mbt ligands are parallel to each other. It should be noted that dimer pairs in **9** are combined by S…S interactions in infinitive chains. The S…S distances are 3.455 and 3.655 Å that is some shorter than sum of van der Waals radii for these atoms ($R(S)_{vdw}$=1.85 Å[24]).

Photophysical properties

With exception of derivatives **4**, **5**, **6** all the complexes demonstrate luminescence in solid state under excitation with λ_{ex} = 360 nm (Fig. 3a-e). It was found that **1** and **2** generate intensive metal-centered emission in the NIR range at 902, 1075 and 1360 nm which can be assigned to $^4F_{3/2} \rightarrow {}^4I_J$ (J = 9/2, 11/2, 13/2) f-f transitions of Nd^{3+} ion. PL spectra of Sm compound **3** consist of broad band of ligand-centered emission at 500 nm along with a set of Sm^{3+} emission bands in visible and NIR region: 565, 604, 650, 707 nm corresponding to $^4G_{5/2} \rightarrow {}^6H_J$ (J = 5/2, 7/2, 9/2, 11/2) transitions and 940, 1020, 1160 nm assigned to $^4G_{5/2} \rightarrow {}^6F_J$ (J = 5/2, 7/2, 9/2) ones

respectively. In the case of ytterbium organolanthanides (**8**, **9**) surprisingly bright NIR irradiation was detected. Their spectra are quite similar and contain poorly resolved peaks of transitions between Stark sublevels of excited $^2F_{5/2}$ and ground $^2F_{7/2}$ states of Yb^{3+} ion. It is interesting to note than **1** and **2** do not reveal any changes in PL at low temperature (77 K) while metal-centered emission of Sm and Yb derivatives becomes stronger and weaker respectively. In contrast to **9** compound **8** demonstrates low temperature PL consisting of four fine-resolved sharp peaks. This feature should be governed by differences in molecular structure and crystal packing of the compounds. Close packing of ester derivative **9** prevents significant thermally activated vibrations but in the case of lower density THF complex **8** vibration amplitude is strongly influenced by temperature. It leads to fine resolution of Stark splitting lines at 77 K in PL spectrum of **8**. The lifetimes of the bands at 1075 nm (**1**), 650 nm (**3**), and 1020 nm (**8**) were found to be 1.6, 14.6, and 5.46 μs, respectively. This is consistent with the data available for other complexes of the same Ln^{3+} ions. Europium and samarium complexes **4**, **5**, **6** exhibit no luminescence at room and low temperatures. These data in the case of **5** are in contradiction to our previous report.[18] Assuming that the partial hydrolysis of **5** can be reason of changing its PL properties it was exposed on air. Indeed the product obtained by hydrolysis has beige colour and reveals characteristic for Eu^{3+} ion luminescence.

To investigate in detail energy transfer processes which occur under photoexcitation in the complexes **1-6**, **8** and **9** energies of $^1S_1$, $^3T_1$ and possible LMCT excited states were defined. Triplet state energy was calculated from short-wavelength shoulder of low temperature phosphorescence spectrum of Gd derivative **7** and equals to 20400 cm^{-1}. Thus, the resonant levels of Nd^{3+} ($^4G_{5/2}$, 17200 cm^{-1}), Sm^{3+} ($^4G_{5/2}$, 17700 cm^{-1}), and Eu^{3+} ($^5D_0$, 17250 cm^{-1}) are appropriate for efficient energy transfer from mbt ligand to lanthanide ion as 2500 $cm^{-1} \leq \Delta E(^3T^*\text{-}Ln^*) \leq 3500$ cm^{-1} equation is valid. This approach describes well PL properties of **1-3** but stays inapplicable to explain the absence of luminescence in the case of **4-5** as well as bright emission of ytterbium complexes **8** and **9**.

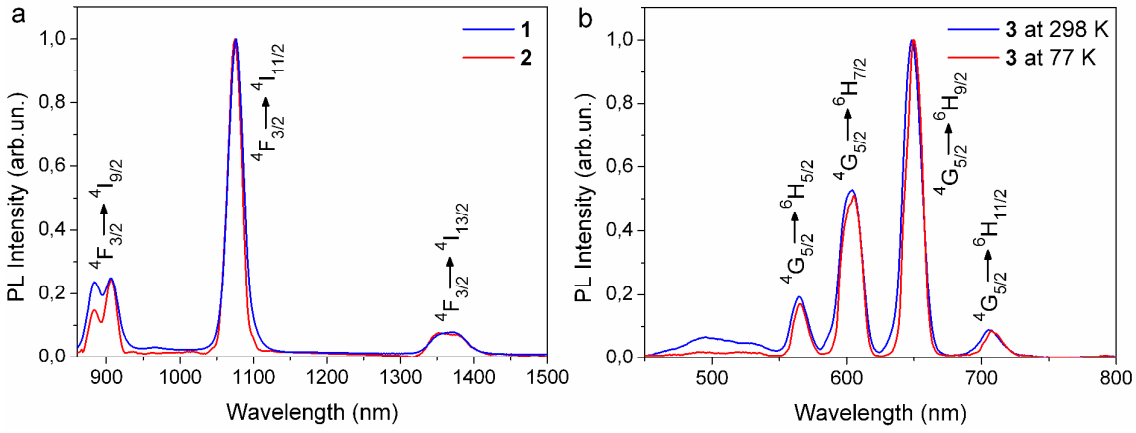

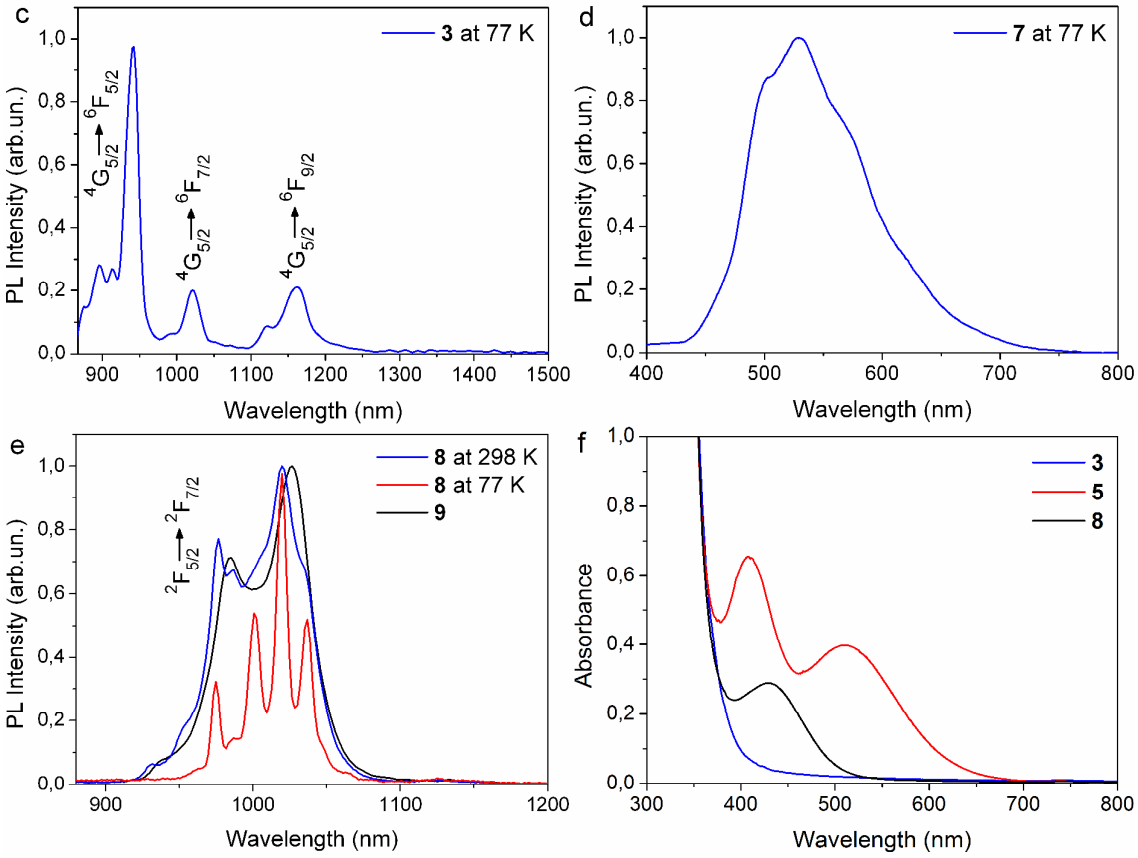

Fig. 3. PL spectra of **1-3** and **7-9** at 298 and 77 K (a-e); absorption spectra of **3**, **5** and **8** (f).

In the meanwhile, LMCT excited state can play significant role in energy transfer process and should be taken into account when energy pathways are considered. It was found that 2-mercaptobenzothiazolate ligand readily forms charge-transfer (CT) complexes with "transition" lanthanides. Observed LMCT absorption bands with the maximum at 530 and 430 nm for Eu (**5**) and Yb (**8**) compounds in THF solution respectively were approximately two orders of magnitude lower than π→π* transition band at 320 nm (Fig. 3f). The energy difference (0.55 eV) between LMCT states of **8** and **5** is comparable with the value of difference of Ln^{3+}/Ln^{2+} electrode potentials in acetonitrile (0.7 V)[25] multiplied by electron charge. Based on the differences between Yb^{3+}/Yb^{2+} and Nd^{3+}/Nd^{2+} [15] or Sm^{3+}/Sm^{2+} [25] potentials absorption maxima of LMCT states for Nd (**1**) and Sm (**3**) mercaptobenzothiazolates can be found at 290 and 374 nm correspondingly, thereby they are hard observable due to overlapping with strong π→π* absorption band of the ligand (Fig. 3f). Unfortunately, absorption spectra of the ester-containing products **2**, **4**, **6** and **9** were not measured because they are insoluble in ester and can be easy solvated by molecules of other polar solvent. However changing of $Ln(mbt)_3(Et_2O)$ (Ln = Sm, Eu, Yb) colours with respect to $Ln(mbt)_3(THF)_2$ ones should reflect the red shift of LMCT absorption bands in the spectra. The excited $^1S_1$ and LMCT levels for **1**, **3**, **5** and **8** were defined

from experimental and predicted long-wavelength absorption edges and depicted on energy diagram (Fig. 4).

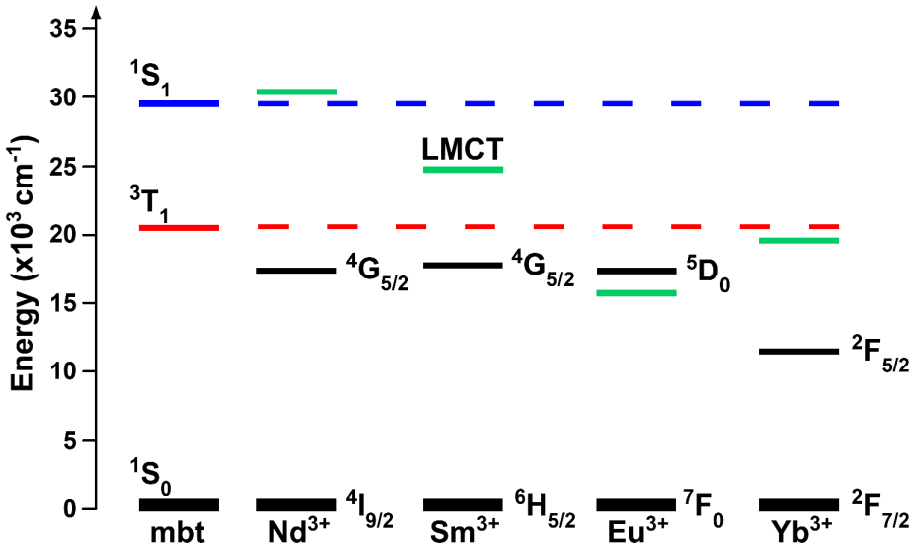

Fig. 4. Energy level diagram for complexes **1**, **3**, **5** and **8**

As shown in Fig. 4 LMCT energy level for **1** lies above $^1S_1$ level of mbt ligand and can not significantly affect to luminescence of Nd^{3+} ion. The lowering of LMCT level in case of samarium derivative **3** leads to formation of energy dissipation pathway characterized by LMCT → $^1S_0$ nonradiative relaxation. Since $^1S_1$ → LMCT electron transition is thermo-activated process Sm^{3+} metal-centered emission increases at low temperature. At first sight the absence of Eu^{3+} luminescence in **5** and **6** is also related to electron nonradiative relaxation from LMCT state which lies even lower than $^3T_1$ level but then intensive emission of Yb compounds **8** and **9** remains inexplicable**.** It should be noted that classical mechanisms described by equations (1)-(3) do not explain this phenomena too. We believe that sensitization of Yb^{3+} luminescence in mercaptobenzothiazolates **8** and **9** occurs due to realization of redox mechanism involving photoinduced intermolecular electron transfer (ET) process.[13] The key point of this mechanism is intramolecular reduction of Yb^{3+} to Yb^{2+} owing to ET from the excited anionic ligand $(L^-)^*$ to Yb^{3+} and back ET from Yb^{2+} to radical species (L•).[26] The possibility of this transformation is stipulated by the relatively low redox potential of Yb^{3+}/Yb^{2+} (Ep = –1.18 V). As a result of the reverse ET from Yb^{2+} to (L•) the anionic ligand (L^-) and the Yb^{3+} cation in the ground $^2F_{7/2}$ or excited $^2F_{5/2}$ state form. Radiative relaxation of $^2F_{5/2}$ state is accompanied by the characteristic emission in NIR region. Obviously, decreasing of Yb^{3+} luminescence at low temperature in **8** and **9** is caused by decreasing rate of the initial reduction process. Moreover this redox mechanism describes adequately the lack of Eu^{3+} emission in the complexes **5** and **6**. The Eu^{3+} cation is readily reduced to Eu^{2+} (Ep = –0.34 V) and, likewise in the case of Yb, under photoexcitation of Eu compounds the intermediate system comprising Eu^{2+} ion and the radical (L•) forms. The

energy of this system is lower than that of upper-lying $^5D_0$ emission level of Eu^{3+}. As a result, the Eu^{3+} cation in **5** and **6** effectively quenches the ligand luminescence and does not reveal metal-centered emission. It should be mentioned that considered redox mechanism opens new perspectives in molecular design of high luminescent organolanthanide materials as ligands which are capable to reduce some trivalent lanthanides having relatively stable Ln^{2+} form (Sm, Tm, Yb) can be synthesized.

Conclusion

In conclusion, the complexes of Nd, Sm, Eu, Gd and Yb with 2-mercaptobenzothaizolate ligands were synthesized. The ester-containing derivative $Yb(mbt)_3(Et_2O)$ was structurally characterized. Investigation of photophysical properties of the compounds obtained revealed that under photoexcitation Nd (**1**, **2**) and Yb (**8**, **9**) complexes exhibit bright NIR metal-centered emission while $Sm(mbt)_3(THF)_2$ (**3**) demonstrates characteristic for Sm^{3+} ion visible and NIR luminescence of high and moderate intensity, respectively. On the contrary $Sm(mbt)_3(Et_2O)$ (**4**) as well as europium derivatives (**5**, **6**) do not generate any emission. Also, different temperature dependences of irradiation intensity were detected for Sm (**3**) and Yb (**8**, **9**) mercaptobenzothiazolates. Based on PL and absorption data different excitation mechanisms of Ln^{3+} in studied complexes were considered: i) classical mechanism with $^3T_1 \rightarrow Ln^{3+}$* energy transfer; ii) classical mechanism involving the additional energy dissipative pathway $^1S_1 \rightarrow$ LMCT $\rightarrow {}^1S_0$; iii) unconventional excitation mechanism which includes the reversible reduction of Ln^{3+} to Ln^{2+}. We suppose that the former one is responsible for PL properties of **5**, **6**, **8** and **9**. Undoubtedly, redox excitation mechanism of some Ln^{3+} ions (Sm^{3+}, Tm^{3+}, Yb^{3+}) opens new perspectives in synthesis of high luminescent organolanthanide materials. This study is now in progress.

Acknowledgment

Work is performed with financial support of the fund competitive support students, post graduate students and young scientific - teaching staff Lobachevsky Nizhny Novgorod State University and supported partially by the grant (the agreement of August 27, 2013 № 02.B.49.21.0003 between The Ministry of education and science of the Russian Federation and Lobachevsky State University of Nizhni Novgorod) and RFBR (project № 13-03-97046).

References

1. M. A. Katkova, A. G. Vitukhnovsky and M. N. Bochkarev, *Usp. Khim.*, 2005, **74**, 1193-1215.
2. J.-C. G. Bunzli, S. Comby, A.-S. Chauvin and C. D. B. Vandevyver, *J. Rare Earth.*, 2007, **25**, 257-274.
3. S. V. Eliseeva and J.-C. G. Bunzli, *Chem. Soc. Rev.*, 2010, **39**, 189-227.
4. J.-C. G. Bunzli and S. V. Eliseeva, *New J. Chem.*, 2011, **35**, 1165-1176.
5. S. I. Weissman, *J. Chem. Phys.*, 1942, **10**, 214-217.
6. E. Nakazawa, *Phosphor Handbook. Second Edition*, CRC Press, Boca Raton, 2007, pp. 123-134
7. J.-C. G. Bunzli and S. V. Eliseeva, *Springer Series on Fluorescence. Lanthanide Luminescence: Photophysical, Analytical and Biological Aspects*, Springer Verlag, Berlin, 2011, vol. 7, pp. 1-45.
8. G. F. de Sa, O. L. Malta, C. de Mello Donega, A. M. Simas, R. L. Longo, P. A. Santa-Cruz and E. F. da Silva Jr., *Coord. Chem. Rev.*, 2000, **196**, 165-195.
9. S. Faulkner, L. S. Natrajan, W. S. Perry and D. Sykes, *Dalton Trans.* 2009, 3890-3899.
10. S. Biju, Y. K. Eom, J.-C. G. Bunzli and H. K. Kim, *J. Mater. Chem. C*, 2013, **1**, 6935-6944.
11. Z. Li, H. Zhang and J. Yu, *Thin Solid Films*, 2012, **520**, 3663-3667.
12. C. Reinhard and H. U. Gudel, *Inorg. Chem.*, 2002, **41**, 1048-1055.
13. W. D. Horrocks Jr., P. J. Bolender, W. D. Smith and R. M. Supkowski, *J. Am. Chem. Soc.*, 1997, **119**, 5972-5973.
14. F. Pointillart, T. Cauchy, O. Maury, Y. Le Gal, S. Golhen, O. Cador and L. Ouahab, *Chem. Eur. J.*, 2010, **16**, 11926-11941.
15. N. Mikheev, *Inorg. Chim. Acta*, 1984, **94**, 241-248.
16. A. Vogler and H. Kunkley, *Comments Inorg. Chem.*, 1997, **19**, 283-306.
17. D. C. Bradley, J. S. Ghotra and F. A. Hart, *J. Chem. Soc. Dalt. Trans.*, 1973, 1021-1023.
18. M. A. Katkova, A. V. Borisov, G. K. Fukin, E. V. Baranov, A. S. Averyushkin, A. G. Vitukhnovsky and M. N. Bochkarev, *Inorg. Chim. Acta*, 2006, **359**, 4289-4296.
19. G. M. Sheldrick (2000). SHELXTL v. 6.12, Structure Determination Software Suite, Bruker AXS, Madison, Wisconsin, USA.
20. SCALE3 ABSPACK: Empirical absorption correction, CrysAlis Pro – Software Package, Agilent Technologies (2012)
21. V. A. Ilichev, M. A. Katkova, S. Yu. Ketkov, N. A. Isachenkov, A. N. Konev, G. K. Fukin and M. N. Bochkarev, *Polyhedron*, 2010, **29**, 400-404.

22. M. A. Katkova, V. A. Ilichev, A. N. Konev, I. I. Pestova, G. K. Fukin and M. N. Bochkarev, *Org. Elec.*, 2009, **10**, 623-630.
23. R. D. Shannon, *Acta Cryst.*, 1976, **A32**, 751-767.
24. S. S. Batsanov, *Russ. J. Inorg. Chem.*, 1991, **36**, 1694-1706.
25. E. J. Cokal and E. N. Wise, *J. Electroanal. Chem.*, 1966, **11**, 406-415.
26. A. P. Pushkarev, V. A. Ilichev, T. V. Balashova, D. L. Vorozhtsov, M. E. Burin, D. M. Kuzyaev, G. K. Fukin, B. A. Andreev, D. I. Kryzhkov, A. N. Yablonskiy and M. N. Bochkarev, *Russ. Chem. Bull.*, 2013, 392-397.